Nuclear Instruments and Methods in Physics Research A 456 (2000) 121–125

NUCLEAR INSTRUMENTS & METHODS IN PHYSICS RESEARCH Section A

www.elsevier.nl/locate/nima

Results from the analysis of data collected with a 50 m^2 RPC carpet at YangBaJing

C. Bacci[a], K.Z. Bao[b], F. Barone[c], B. Bartoli[c], P. Bernardini[d], S. Bussino[a], E. Calloni[c], B.Y. Cao[e], R. Cardarelli[f], S. Catalanotti[c], A. Cavaliere[f], S. Cavaliere[c], F. Cesaroni[d], P. Creti[a], Danzengluobu[g], B. D'Ettorre Piazzoli[c], M. De Vincenzi[a], T. Di Girolamo[c], G. Di Sciascio[c], Z.Y. Feng[h], Y. Fu[e], X.Y. Gao[i], Q.X. Geng[i], H.W. Guo[g], H.H. He[j], M. He[e], Q. Huang[h], M. Iacovacci[c], N. Iucci[a], H.Y. Jai[h], F.M. Kong[e], H.H. Kuang[j], Labaciren[g], B. Li[b], J.Y. Li[e], Z.Q. Liu[i], H. Lu[j], X.H. Ma[j], G. Mancarella[d], S.M. Mari[k], G. Marsella[d], D. Martello[d], D.M. Mei[g], X.R. Meng[g], L. Milano[c], J. Mu[i], M. Panareo[d], G. Pellizzoni[a], Z.R. Peng[j], C. Pinto[d], P. Pistilli[a], E. Reali[f], R. Santonico[f], C. Sbarra[l], P.R. Shen[j], C. Stanescu[a], J. Su[j], L.R. Sun[b], S.C. Sun[b], A. Surdo[d,*], Y.H. Tan[j], S. Vernetto[m], C.R. Wang[e], H. Wang[j], H.Y. Wang[j], Y.N. Wei[b], H.T. Yang[j], Q.K. Yao[b], G.C. Yu[h], X.D. Yue[b], A.F. Yuan[g], H.M. Zhang[j], J.L. Zhang[j], N.J. Zhang[e], T.J. Zhang[i], X.Y. Zhang[e], Zhaxisangzhu[g], Zhaxiciren[g], Q.Q. Zhu[j]

[a]*INFN and Dipartimento di Fisica dell'Università di Roma Tre, Italy*
[b]*Zhenghou University, Henan, China*
[c]*INFN and Dipartimento di Fisica dell'Università di Napoli, Italy*
[d]*INFN Sezione di Lecce and Dipartimento di Fisica dell'Università di Lecce, Italy*
[e]*Shangdong University, Jinan, China*
[f]*INFN and Dipartimento di Fisica dell'Università di Roma "Tor Vergata", Italy*
[g]*Tibet University, Lhasa, China*
[h]*South West Jiaotong University, Chengdu, China*
[i]*Yunnan University, Kunming, China*
[j]*IHEP, Beijing, China*
[k]*Universita della Basilicata, Potenza, Italy*
[l]*Dipartimento di Fisica dell'Università di Padova, Italy*
[m]*Istituto di Cosmogeofisica del CNR and INFN, Torino, Italy*

Abstract

An RPC carpet covering $\sim 10^4\,\mathrm{m}^2$ (ARGO-YBJ experiment) will be installed in the YangBaJing Laboratory (Tibet, People's Republic of China) at an altitude of 4300 m a.s.l. A test-module of $\sim 50\,\mathrm{m}^2$ has been put in operation in this

* Corresponding author.

PII: S0168-9002(00)00976-1

laboratory and about 10^6 air shower events have been collected. The RPC performance at high altitude and the carpet capability of reconstructing the shower features are presented.

1. Introduction

The ARGO-YBJ experiment will be installed at YangBaJing High Altitude Cosmic Ray Laboratory (4300 m a.s.l., 606 g/cm^2), 90 km North to Lhasa (Tibet, People's Republic of China). A major aim of the experiment is the study of cosmic rays at an energy threshold of ~ 100 GeV, by detecting small size air showers. The apparatus consists of a full coverage detector of dimension $\sim 71 \times 74\,m^2$ made by a single layer of Resistive Plate Counters (RPCs), surrounded by a guard ring partially ($\sim 50\%$) instrumented with RPCs. A lead converter 0.5 cm thick will cover uniformly the RPC plane in order to increase the number of charged particles and to reduce the time spread of the shower front. The operation at very high altitude and the full coverage detector technique permit to achieve an energy threshold lower than conventional air shower arrays, allowing to bridge the GeV and TeV energy regions and to face a wide range of fundamental issues in Cosmic Ray and Astroparticle Physics including γ-ray astronomy, GRBs physics and the measurement of the $\bar{p}/p$ at TeV energies [1]. In order to investigate both the RPCs performance at 4300 m a.s.l. and the capability of the detector to sample the shower front of atmospheric cascades, during 1998 a full coverage carpet of $\sim 50\,m^2$ has been put in operation in the YangBaJing (YBJ) Laboratory. Details of the results can be found in Refs. [2,3].

2. The experimental set-up

The detector set-up is an array of 3×5 chambers of area $280 \times 112\,cm^2$ each, covering a total area of $\sim 8.6 \times 6.0\,m^2$. The active area corresponds to a $\sim 89\%$ coverage. The RPCs, with a 2 mm gas gap, are built with bakelite electrode plates of volume resistivity in the range (0.5–1) 10^{12} Ω cm. The RPC signals are picked up by means of aluminium strips 3.3 cm wide and 56 cm long which are glued on a 0.2 mm thick film of poly-ethylene-tereftalate (PET). A grounded aluminium foil is used to shield the bottom face of the RPC. The front–end circuit contains 16 discriminators, with about 50 mV voltage threshold, and provides a FAST-OR signal with the same input-to-output delay (10 ns) for all channels. The 16 strips connected to the same front–end board are logically organized in a pad of $56 \times 56\,cm^2$ area. The pad is the basic element ("pixel") which defines the space–time pattern of the shower. The triggered times are read out by means of multihit TDCs (with 1 ns time bin) operated in COMMON STOP mode. The set-up was completed with a small telescope consisting of 3 RPCs of $50 \times 50\,cm^2$ area and the triple coincidence of their FAST-OR signals was used to define a cosmic ray crossing the telescope.

3. RPC performance

The RPCs were operated in streamer mode. This mode delivers large-amplitude saturated signals and is less sensitive than the avalanche or proportional mode to electromagnetic noise, changes in the environment conditions and mechanical deformations of the detector. Three gas mixtures were tested which used the same components (argon, isobutane and tetrafluoroethane) in different proportions: TFE/Ar/i-But = 45/45/10, 60/27/13 and 75/15/10. A higher concentration of TFE in place of Ar increases the primary ionization thus compensating for the 40% reduction due to the lower gas pressure (600 mbar) at YBJ and reduces the afterpulse probability. The detection efficiency vs. the operating voltage for the three gases was measured for the RPC in the central position of the trigger telescope (RPC2 in the following) and is shown in Fig. 1. The data are consistent with an increase of 30–40 V in the operating voltage for a 1% reduction of the Argon concentration. In spite of the different operating voltages all three gases approach the same efficiency of about 90% which

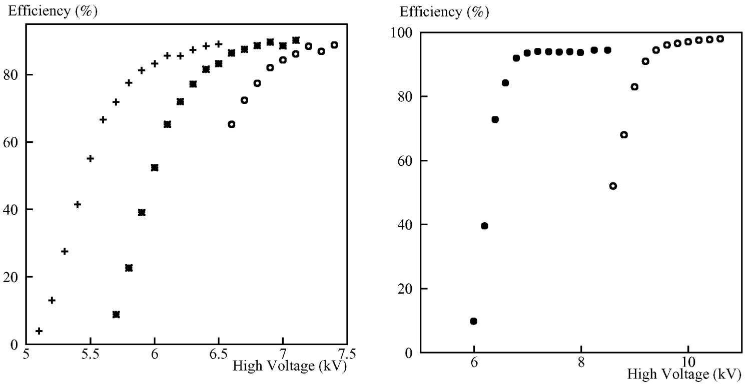

Fig. 1. Left: detection efficiency of one RPC of the auxiliary telescope vs. operating voltage for three gas mixtures: TFE/Ar/i-But = 45/45/10 (+); 60/27/13 (∗) and 75/15/10 (○). Right: detection efficiency vs. operating voltage for one of the carpet RPCs (●) [TFE/Ar/i-But = 75/15/10]. The same curve for a 2 mm gap RPC operating at sea level is also reported (○) for comparison.

includes the inefficiency due to geometrical effects. Since the charge per count delivered in the RPC gas is decreasing with increasing TFE fraction, we decided to operate the test carpet with the gas mixture TFE/Ar/i-But = 75/15/10 (charge per count ~0.4 nA), in order to extend the dynamic range achievable for the analogical read-out. The operating efficiency for 4 OR-ed pads of one RPC is shown in Fig. 1. The efficiency was measured using cosmic ray signals defined by the triple coincidence of the telescope placed at the center of the four pads. The same curve for a 2 mm gap RPC operated at sea level is also shown for comparison. It results that the plateau efficiency measured at YBJ is 3–4% lower than at sea level. That is attributed to a contamination from soft particles not completely eliminated (see Ref. [2] for a discussion about this point). A rather flat singles rate plateau is observed corresponding to a rate of about 400 Hz for a single $56 \times 56\ \mathrm{cm}^2$ pad. The time jitter distributions of the pad signals were obtained by measuring the delay of the FAST-OR signal with respect to RPC2 in the trigger telescope. The standard deviations of such distributions indicate a resolution of 1.0 ns for the single RPC.

4. Shower data and analysis results

A trigger based on pad multiplicity has been used to collect $\sim 10^6$ shower events in April–May 1998. Data were taken either with or without a 0.5 cm layer of lead on the whole carpet to investigate the converter effect on multiplicity and angular resolution. The integral rate as a function of the pad multiplicity is shown in Fig. 2 for showers before and after lead installation. These data have been used firstly to define the calibration procedures and then analyzed to study shower properties, primarily the zenith angle distribution and the density spectrum. A detailed account is given in Ref. [3]. Here we report results concerning the time distribution of particles on the shower front and the detector angular resolution.

Due to the reduced detector size, the time profile of the sampled shower front is expected to exhibit a planar shape, so that the particle arrival times can be fitted by a linear function of the positions. In this approximation, the distribution of the shower particle time residuals with respect to the fitted plane is shown in Fig. 2 (right plot) for quasi-vertical events ($\theta < 15^\circ$), in two different multiplicity ranges. The long tail is due to particles delayed with respect to the shower front. For low multiplicity events the width of this distribution is a measurement of the shower thickness, while for high multiplicity events the spread σ is related to the fluctuations of the first particle detected by each pad. Taking into account the total detector resolution of 1.3 ns (due to RPC intrinsic jitter, strip length, electronics time resolution) the time jitter of the earliest particles in high multiplicity events is ~ 0.9 ns.

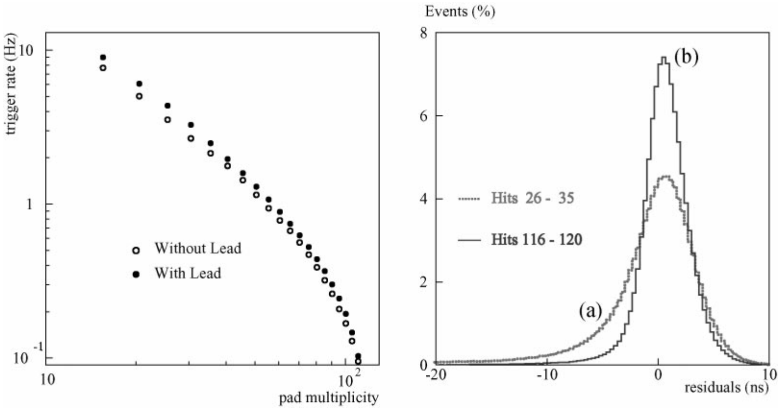

Fig. 2. Left: the integral event rate as a function of the pad multiplicity. Right: time residual distribution for events with different pad multiplicity (all channels added).

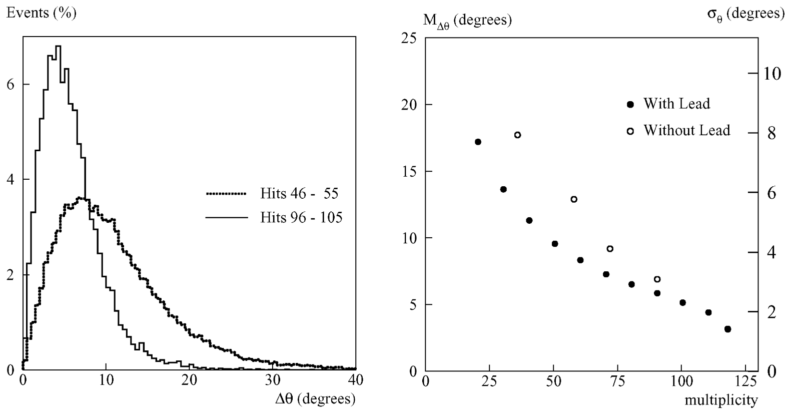

Fig. 3. Even–odd angle difference distribution for events with different pad multiplicity and median of $\Delta\theta$ distribution (or angular resolution σ_θ) as a function of pad multiplicity.

The angular resolution of the carpet was estimated by dividing the detector into two independent sub-arrays ("odd pads" and "even pads") and comparing the two reconstructed shower directions. Events with total number of hits $N_{\rm hit}$ were selected according to the constraint $N_{\rm odd} \simeq N_{\rm even} \simeq N_{\rm hit}/2$. The distribution of the even–odd angle difference $\Delta\theta$ is shown in Fig. 3 for events in different multiplicity ranges and $\theta < 55^\circ$. These distributions narrow, as expected, with increasing shower size.

The effect of the lead sheet on the angular resolution can be appreciated in the right plot of Fig. 3, where the median $M_{\Delta\theta}$ of the distribution of $\Delta\theta$ as a function of pad multiplicity, for showers reconstructed with and without the lead, is shown. The improvement of the angular resolution is a factor ~ 1.4 for $N_{\rm hit} = 50$ and decreases with increasing multiplicity. Assuming that the angular resolution function for the entire array is a Gaussian, its standard deviation is given by [4] $\sigma_\theta = M_{\Delta\theta}/(1.177 \times 2)$. This chessboard method yields a standard deviation $\sigma_\theta \sim 2^\circ$ for events with a pad multiplicity $\geqslant 100$. We note that, according to MC simulations, these events would be recorded by ARGO-YBJ with a hit multiplicity > 1000 over distances of the order of 50 m or more.

5. Conclusions

A carpet of $\sim 50\,m^2$ of RPCs has been put in operation at the YangBaJing Laboratory in order to study the high-altitude performance of RPCs and the detector capability of imaging with high granularity a small portion of the EAS disc, in view of an enlarged use in Tibet (ARGO-YBJ experiment). The results of this test confirm that RPCs can be operated efficiently ($\geqslant 95\%$) to sample air showers at high altitude with excellent time resolution (~ 1 ns). The analysis of data collected with a shower trigger suggests that the RPCs carpet capability of reconstructing the shower features is consistent with expectations. As a conclusion, the overall results of the test look well promising for future operation of the full detector.

References

[1] M. Abbrescia et al., Astroparticle Physics with ARGO, Proposal, 1996.
[2] C. Bacci et al., Nucl. Instr. and Meth. A 443 (2000) 342.
[3] C. Bacci et al., Results from the ARGO-YBJ test experiment, Astropart. Phys., submitted for publication.
[4] D.E. Alexandreas et al., Nucl. Instr. and Meth. A 311 (1992) 350.